CDK6 ACTIVITY IN A RECURRING CONVERGENT KINASE NETWORK MOTIF

Christina Gangemi[a,b], Rahkesh T Sabapathy[c] & Harald Janovjak[a,b,c]

[a] Australian Regenerative Medicine Institute (ARMI), Faculty of Medicine, Nursing and Health Sciences, Monash University, 3800 Clayton/Melbourne, Victoria, Australia

[b] European Molecular Biology Laboratory Australia (EMBL Australia), Monash University, 3800 Clayton/Melbourne, Victoria, Australia

[c] Flinders Health and Medical Research Institute, College of Medicine and Public Health, Flinders University, 5042 Bedford Park/Adelaide, South Australia, Australia

To whom correspondence should be addressed: harald.janovjak@flinders.edu.au.

Keywords: Kinase, signaling network, inhibitor, protein engineering, convergence

ABSTRACT

More than 500 kinases phosphorylate ~15% of all human proteins. The architecture of the phosphorylation network has been studied extensively, for instance to compile global interaction maps, trace signal transduction pathways or identify chemical intervention points. In contrast, systematic investigation of local motifs is rare but may provide a complementary understanding of network and kinase function. Here, we report on the occurrence, topology and experimental analysis of convergent kinase-substrate relationships (cKSRs) in which ≥two kinases phosphorylate the same substrate. Through bioinformatics analysis we found that human cKSRs are frequent and involve >80% of all kinases and >24% of all substrates. We show that cKSRs occur over a wide range of stoichiometries harnessing converging kinases that are in many instances recruited from the same family subgroup and co-expressed. Experimentally, we demonstrate at the prototypical convergent CDK4/6 kinase pair how multiple inputs at the major tumor suppressor retinoblastoma protein (RB) can hamper *in situ* analysis of individual kinases. We hypothesized that overexpression of one kinase combined with a CDK4/6 inhibitor can dissect convergence. In breast cancer cells that express high levels of CDK4, we confirmed this hypothesis and developed a high throughput compatible assay that sensitively quantifies genetically modified CDK6 variants and small molecule or protein inhibitors. Collectively, our work provides deeper insights into the phosphorylation network through the identification and analysis of kinase convergence.

INTRODUCTION

Protein phosphorylation is the most common reversible post-translational modification in eukaryotes and an essential regulator of cell and organism physiology in health and disease. Recent experimental analysis of the phosphoproteome has revealed a large number of human protein phosphorylation sites (e.g., >200'000 sites in large mass spectrometry-based datasets, or >10'000 sites in datasets of experimentally validated kinase-substrate interactions) (Aebersold and Mann, 2016; Colinge et al., 2014; Hornbeck et al., 2015; Lemeer and Heck, 2009; Riley and Coon, 2016). The architecture of the emerging phosphorylation network has been studied extensively. Whilst many studies focused on global interaction maps or linear/interconnected signaling pathways (reviewed in (Alganem et al., 2022; Chen and Eschrich, 2014; Colinge *et al.*, 2014)), less attention has been devoted to a network-wide analysis of local motifs (Invergo and Beltrao, 2018). With ~500 kinases and ~3'000 substrate proteins encoded in the human genome, it is expected that each kinase phosphorylates many sites and that on each substrate protein multiple sites are phosphorylated. Nodes in which multiple kinases converge on one substrate (**Fig. 1A, left**) are likely to occur in the network but their number and topologies have not been systematically investigated. These convergent network motifs are of interest not only because of their involvement in biological functions, including signal amplification, pathway crosstalk and feedback loops (**Fig. 1A, right**), but also because they can lead to challenges during experimental interrogation. For instance, quantifying the activity of a kinase *in situ* can be hampered by background phosphorylation of its substrate by additional convergent kinases. Indeed, in well-known cases of convergence, the presence of multiple inputs has resulted in limited experimental methods for functional analysis (see below).

One prototypical case of phosphorylation convergence centers around the CDK4/6 serine (Ser)/threonine (Thr) kinase pair. CDK4/6 and their associated D-type cyclins (CyclinD1/D2/D3) are core components of the cell cycle machinery and regulate commitment to cycle entry (Malumbres and Barbacid, 2001; Sherr and Roberts, 1999). Unbound CDK4/6 are catalytically inactive. Assembled active CDK4/6-D-type cyclin complexes are regulated positively (e.g., by the CDK-activating complex (Fisher, 2005; Schachter et al., 2013)), negatively (e.g., by INK4 proteins (Hirai et al., 1995; Parry et al., 1999; Sherr and Roberts, 1999)), as well as positively or negatively in a context dependent manner (e.g., by KIP proteins (Blain, 2008; Cheng et al., 1999; Parry *et al.*, 1999; Sherr and Roberts, 1999)). Within the cell cycle, CDK4/6 phosphorylate key regulatory sites on the major growth suppressor RB (Kaelin, 1999; Rubin, 2013). RB scavenges E2F transcription factors that are required for cell cycle progression and phosphorylation by various cyclins releases this interaction. Whilst their roles in the cell cycle and in many cases their substrate specificity are overlapping (Malumbres et al., 2004), CDK4/6 also have non-overlapping kinase activity-dependent and -independent functions outside of the cell cycle (Anders et al., 2011; Dall'Acqua et al., 2017; Hydbring et al., 2016; Tigan et al., 2016; Wang et al., 2017). Not surprisingly, CDK4/6 have received attention as major drivers of cancer and are targeted using small molecule inhibitors (Malumbres, 2014; Sherr et al., 2016). However, the absence of inhibitors that are specific for either kinase and their overlapping activity can challenge experimental analysis.

As shown previously, the presence of either CDK4 or CDK6 is sufficient to phosphorylate RB to levels that prohibit analysis of the activity of the other kinase (Malumbres *et al.*, 2004; Yang et al., 2017). As a consequence, CDK4 and CDK6, in particular in the context of RB phosphorylation, are commonly functionally assayed *in vitro,* either using purified kinases and substrates, such as a recombinant RB fragment (Bockstaele et al., 2006; Jinno et al., 1999; Kitagawa et al., 1996; Paternot et al., 2003), or after immunoprecipitation (Bockstaele et al., 2009; Bockstaele *et al.*, 2006). More recently, fluorescent biosensors of CDKs were developed but these require substrate-specific chemically-functionalized polypeptide probes and have not been deployed in living cells (Pellerano and Morris, 2021; Soamalala et al., 2020; Van et al., 2014). In cells, exploration of potential CDK6 substrates was conducted using gel-based electrophoretic

106 migration shift assays that do not offer high throughput and may not in all cases provide the
107 resolution required to visualize phosphorylation events (Anders *et al.*, 2011). Finally,
108 transcriptional reporter plasmids for signals downstream of RB often exhibit low signal-to-noise
109 ratios (Budde et al., 2005; Chen et al., 1996a; Chen et al., 1996b). Collectively, assaying the
110 CDK4/6-RB-axis in complex cellular environments and compatible with parallelization is currently
111 challenging. Because of its biological/biomedical significance and these experimental limitations,
112 the CDK4/6 pair represents an interesting test case for experimental convergence analysis.

113 Here, we first performed a network-wide analysis of local kinase-substrate interactions
114 with a focus on cKSRs. We quantified their frequency, topology and kinase family subgroup
115 distribution. We hypothesized that kinase overexpression combined with the use of a CDK4/6
116 inhibitor provides an approach to assay an individual kinase of the pair. Using this strategy, we
117 were able to characterize genetically modified CDK6s and their inhibitors in breast cancer cells
118 expressing high levels of CDK4. Collectively, our work reveals fundamental properties of cKSRs
119 and demonstrates a possible approach to dissect convergence in cellular contexts even in the
120 absence of kinase-specific inhibitors.

121

122

123 MATERIALS AND METHODS

124 *Key resources table*

REAGENT or RESOURCE	SOURCE	IDENTIFIER
Reagents		
Abemaciclib (LY2835219)	AdooQ Bioscience	A12989
Ribociclib (LEE011)	Selleckchem	S7440
MEM	Gibco	11095080
Penicillin streptomycin	Gibco	15140122
FBS	Gibco	26140079
Insulin, recombinant human zinc solution	Gibco	12585014
PBS	Gibco	20012050
Opti-MEM	Gibco	31985070
X-tremeGENE HP DNA Transfection Reagent	Roche	6366236001
Cell Lysis Buffer (10x)	Cell Signalling Technology	9803S
Glycerol	Sigma-Aldrich	G5516-500ML
SDS	Sigma-Aldrich	L3771-500G
Bromophenol blue	Sigma-Aldrich	B0126-25G
β-mercaptoethanol	Sigma-Aldrich	M3148-25ML
20x Bolt MOPS SDS Running Buffer	Invitrogen	B0001
Bolt 4-12% Bis-Tris Plus Gels 15-well	Invitrogen	NW04125BOX
Immun-Blot PVDF Membrane	Bio-Rad	1620177
BSA	Sigma-Aldrich	A7906-50G
Tween 20	Sigma-Aldrich	P1379
Clarity Western ECL Substrate	Bio-Rad	1705060
Antibodies		
DYKDDDDK Tag (D6W5B) Rabbit mAb (FLAG-Tag)	Cell Signaling Technology	14793

GAPDH (D16H11) XP Rabbit mAb	Cell Signaling Technology	5174
HA-Tag (C29F4) Rabbit mAb	Cell Signaling Technology	3724
Phospho-RB (Ser780) (D59B7) Rabbit mAb	Cell Signaling Technology	8180
RB (4H1) Mouse mAb	Cell Signaling Technology	9309
Goat Anti-Mouse IgG (H+L)-HRP Conjugate	Bio-Rad	1721011
Goat Anti-Rabbit IgG (H + L)-HRP Conjugate	Bio-Rad	1706515
Kits		
AlphaLISA SureFire Ultra p-RB (Ser780)	PerkinElmer	ALSU-PRB-C
AlphaLISA SureFire Ultra RB Total	PerkinElmer	ALSU-TRB-A

KSR analysis

The KSR analysis was based on a comprehensive set of experimentally determined phosphorylation sites deposited in PhosphoSitePlus (PSP) (Hornbeck *et al.*, 2015). PSP is extensive and continuously manually-curated. Phosphorylation sites were downloaded (http://www.phosphosite.org, v6.6.0.2, February 2022) and further processed to obtain cKSRs using custom macros and formulas.

The first analysis was substrate-centric. This analysis was performed for Ser/Thr and tyrosine (Tyr) phosphorylation events separately and by considering either *general* cKSRs (i.e., ≥two kinases phosphorylate the same substrate but not necessarily at the same site) or *site-specific* cKSRs (i.e., ≥two kinases phosphorylate the same substrate at the same phosphorylation site). First, PSP sites were limited to human substrate entries. Second, to eliminate duplicate pairings of kinases and substrates/sites for accurate counting, fingerprints were calculated that combined the kinase and substrate/site name (e.g., “CDK4:RB” or “CDK4:RB:S780”). In a third step, the fingerprints were used to identify unique substrates/sites. In a fourth step and for each unique substrate/site, the number of active kinases was counted and their names compiled. For general cKSRs, these unique lists are given in **Supplementary Tables S1 and S2** (Ser/Thr and Tyr phosphorylation, respectively). For site-specific cKSRs, these unique lists are given in **Supplementary Tables S3 and S4** (Ser/Thr and Tyr phosphorylation, respectively). Finally, the occurrence of each possible cKSR of K:1 topology (where K denotes the number of kinases and is between 1 and 50, and 1 denotes the substrate/site) were counted. This analysis also reported on the total number of substrates/sites involved in cKSRs.

The second analysis was kinase-centric. This analysis was performed for Ser/Thr and Tyr kinases separately. Above kinase-substrate pairings were reanalyzed to produce filtered lists of kinases. The main applied filter was to include only those kinases which phosphorylate substrates that are subject to general or site-specific cKSRs (**Supplementary Tables S5-S8**). This list was then further used to retrieve kinase-specific information, such as the number of substrates that is phosphorylated by each kinase.

Kinase family subgroup analysis

Lists containing the kinases that phosphorylate each substrate/site were generated (as in **Supplementary Tables S1-S4**). For each kinase, subgroup information was obtained from KinHub (http://kinhub.org, column: group) after correcting, where necessary and in a small number of cases, kinase nomenclature using the nomenclature list of KinHub. For each set of kinases that act on a specific substrate/site, the occurrence of members of the canonical kinase family subgroups AGC, CAMK, CK1, CMGC, RGC, STE, TK, TKL as well as atypical and “other”

(Manning et al., 2002) was counted and this information encoded in a numeric string. These strings were then analyzed to reveal the number of substrates/sites that are phosphorylated by kinases from multiple family subgroups and the number of substrates/sites that are phosphorylated by ≥two kinases from at least one family subgroup.

Identification of reciprocal phosphorylation loops

Reciprocal phosphorylation loops between two kinases were identified in the general cKSR dataset as follows: First, lists were compiled of all kinases (labelled "A" in **Supplementary Fig. S1**) that are phosphorylated by multiple kinases, e.g. an input kinase and a kinase in the reciprocal loop. Second, for each of these kinases lists of its substrates were compiled. Third, these substrate lists were compared to lists of kinases that phosphorylate kinase A to identify kinases B_1-B_n. Kinase A-B pairs are then compiled in **Supplementary Table S13**. For each identified phosphorylation loop, the WebOfScience database (Clarivate Analytics) was searched with keyword combinations that include the kinases and "feedback loop" or "reciprocal". Occurrence of prior mention of the reciprocal interactions is also indicated in **Supplementary Table S13**.

Co-expression analysis

The co-expression analysis was based on an analysis of 1393 cancer cell lines collected by the cancer cell line encyclopedia initiative (Barretina et al., 2012). Expression data of all protein-coding genes in the $\log_2$(TPM+1) format (where +1 denotes a pseudocount) were downloaded (http://sites.broadinstitute.org/ccle/, http://depmap.org/portal/download/, v22Q1, April 2022,) and further processed using custom macros and formulas. This analysis was performed for Ser/Thr and Tyr phosphorylation events separately and by considering either general or site-specific cKSRs. First, protein names in the expression data were cropped to only contain short HGNC compliant names. Second, the TPM values were converted into a binary format (1: expressed, 0: not expressed) using specified TPM thresholds (5, 10 and 20). Third, lists containing the kinases that phosphorylate each substrate/site were generated (as in **Supplementary Tables S1-S4**). Where necessary and in a small number of cases, kinase nomenclature was corrected using the nomenclature list of KinHub (http://kinhub.org). Fourth, for each group of kinases that act on a substrate/site, the number of cell lines was counted in which ≥two convergent kinases are co-expressed. The percentage was defined as the co-expression score and is compiled in **Supplementary Tables S9-S12**.

Reagents

Reagents utilized are listed in the Key Resources Table. Abemaciclib (LY2835219) (AdooQ Bioscience) was diluted in dimethyl sulfoxide (DMSO) to generate a 2 mM stock solution. Ribociclib (LEE011) (Selleckchem) stock solutions were prepared at 10 mM in DMSO. Inhibitors were further diluted in cell culture media before being added to cells and equivalent amounts of DMSO were added to control wells.

Vectors and constructs

All genes were ordered as synthetic genes (gBlocks, Integrated DNA Technologies) and designed to contain an N-terminal HA-tag (YPYDVPDYA), with the exception of Cyclin D3 that contained an N-terminal FLAG-tag (DYKDDDDK). gBlocks were amplified in polymerase chain reactions using oligonucleotides with restriction site overhangs and digested with the corresponding restriction enzymes. These were NotI and BamHI for wildtype (WT) CDK6 and p18INK4a, XhoI

207 and BamHI for Cyclin D3, NotI and BstEII for CDK6 with N-terminal pdDronpa1, and BstEII and
208 BamHI for CDK6 with internal loop pdDronpa1 (New England Biolabs). pcDNA3.1(-) vector
209 (Thermo Fisher Scientific) was digested with the corresponding enzymes and ligated with
210 amplified genes using T4 DNA ligase (Promega).

211 Single residue mutations were introduced in WT CDK6 using overlapping oligonucleotides
212 designed in PrimerX (https://www.bioinformatics.org/primerx/) using the QuikChange option.
213 Circular PCRs were performed with a high-fidelity polymerase (Q5, NEB) followed by digestion
214 with DpnI restriction enzyme (New England Biolabs).

215 All genes were verified using Sanger sequencing (MicroMon, Monash University). The
216 sequences of the engineered CDK6 fusion proteins are summarized in **Supplementary Table**
217 **S14.**

218

219 *Cell culture*

220 Human breast cancer MCF-7 cells (ATCC, HTB-22) were kindly provided by Antonella Papa
221 (Monash University) and cultured in Minimum Essential Media (MEM, Gibco) in a humidified
222 incubator with 5% CO_2 atmosphere at 37°C. Medium was supplemented with 10% FBS, 0.1 mg/ml
223 human recombinant insulin, 100 U/ml penicillin and 0.1 mg/ml streptomycin (Gibco). Transfections
224 were conducted by seeding 500,000 cells per well in 6-well plates for immunoblotting experiments
225 or 18,000 cells in 96-well plates for AlphaLISA assays. 24 hrs after seeding, cells were transfected
226 with plasmid DNA using X-tremeGENE HP DNA transfection reagent (Roche) as per the
227 manufacturer's protocol using a total vector amount of 2 µg (6-well) or 0.1 µg (96-well). A 3:1 ratio
228 of transfection reagent to DNA; (6 µl:2 µg) for 6-well or (0.3 µl:0.1 µg) for 96-well was used. Single
229 construct controls were supplemented with empty pcDNA3.1(-) vector and for co-expression
230 plasmids were added in a ratio of 1:1 or 1:1:1. Mock transfections contained empty pcDNA3.1(-)
231 vector only. After 24 hrs, the culture medium was replaced and CDK4/6 inhibitor/s added.

232

233 *Immunoblotting*

234 After 24 hrs of inhibitor treatment, cells were transferred onto ice and washed with cold 1x
235 phosphate-buffered saline (PBS). 500 µl of 1x cell lysis buffer (Cell Signalling Technology)
236 supplemented with Complete EDTA-free Protease Inhibitor Cocktail (Roche) was added for cell
237 lysis. Lysates were collected and sonicated for 10 s, followed by incubation at 4°C with constant
238 shaking (2000 rpm) for 30 min. Samples were then centrifuged for 20 min at 4°C before adding
239 4x Laemmli loading buffer (40% glycerol, 240 mM Tris/HCL, pH 6.8, 8% SDS, 0.04%
240 bromophenol blue and 5% β-mercaptoethanol) and denaturation at 95°C for 5 min. Proteins were
241 separated using Bolt 4-12% Bis-Tris Plus Gels (Invitrogen) run at 140 V for 60 min before being
242 transferred onto PVDF membranes (100 V for 100 min) (Bio-Rad). Membranes were blocked in
243 1x TBST (1x Tris-buffered saline, 0.1% Tween) containing 5% skim milk powder for >1 hr at room
244 temperature (rotating). Membranes were then probed with indicated primary antibodies (diluted
245 in either 5% skim milk powder or bovine serum albumin in 1x TBST) overnight whilst rotating at
246 4°C. Corresponding mouse or rabbit horseradish peroxidase-conjugated secondary antibodies
247 (diluted 1:10,000 in 1x TBST) were added for 1 hr at room temperature (Bio-Rad).
248 Chemiluminescence was detected by adding Clarity Western ECL Substrate (1:1 of luminol and
249 peroxide solutions) in a ChemiDoc Touch Imaging System (Bio-Rad).

250

251 *Energy transfer-based assays*

252 AlphaLISA SureFire Ultra assay kits (PerkinElmer) were used in a two-plate two-incubation assay
253 protocol for adherent cells according to manufacturer's instructions. Briefly, cells were washed

with 100 µl of PBS per well, followed by addition of 100 µl of 1x lysis buffer and incubated for 10 min on a plate shaker at 350 rpm. Lysate was transferred to light grey 384-well untreated AlphaPlates (PerkinElmer) by adding 10 µl per well. Both kits were used to run both assays in parallel on the same lysates from each condition. 5 µl of acceptor mix was added per well and incubated for 1 hr in the dark followed by addition of 5 µl of donor mix (under low light conditions) and incubated for a further hour in the dark. Wells were then read using a PHERAstar plate reader (BMG). Each condition was assayed in triplicates per kit.

Data analysis and statistics

Densitometry analysis was performed on immunoblots using ImageLab 6.1 software (Bio-Rad). Kinase-substrate topology analysis was performed using equations and filters in Microsoft Excel. Reciprocal interaction analysis, kinase family analysis and co-expression analysis was performed using macros written in C in Igor Pro 6.22 (Wavemetrics). Data for **Supplementary Fig. S6** was prepared in UniProt (http://www.uniprot.org, alignment of human CDK5 and CDK6) and PyMOL 2.5 (Schrödinger; protein structures: PDB-ID 1JOW for CDK6 and 1H4L for CDK5). All other data was analysed using Prism (9.0, GraphPad).

RESULTS

Convergent motifs are abundant in Ser/Thr and Tyr phosphorylation

We systematically analyzed convergent phosphorylation motifs. As the data source we utilized the comprehensive PSP repository of experimentally determined phosphorylation sites (Hornbeck *et al.*, 2015). >21'000 phosphorylation sites are deposited in PSP across all species, with human being the most prominent substrate type (accounting for 13'916 or 64% of sites). We limited our analysis to these human phosphorylation sites and separated Ser/Thr from Tyr kinase reactions. Using a fingerprinting approach, we identified unique substrates and for each substrate compiled the phosphorylating kinases (**Supplementary Tables S1-S4**). We found that convergent motifs are common both in Ser/Thr and Tyr phosphorylation. Of the 2629 substrates of 350 Ser/Thr kinases, 1268 (48%) are phosphorylated by more than one kinase (**Fig. 1B**). Similarly, in the case of Tyr phosphorylation by 129 kinases, 422 (65%) of 649 substrates are phosphorylated by more than one kinase (**Fig. 1C**). We next determined cKSR topologies expressed as K:1, where K denotes the number of kinases and 1 denotes the substrate. We found that 21, 10 and 6.1% of substrates are phosphorylated by two, three or four Ser/Thr kinases, and the remaining substrates by varying kinase numbers (**Fig. 1B,C**). We also found that 19, 6.6 and 5.2% of substrates are phosphorylated by two, three or four Tyr kinases, and the remaining substrates by varying kinase numbers. Thus, cKSRs are not only generally abundant but also occur with broad topologies that are somewhat comparable between Ser/Thr and Tyr phosphorylation.

The analysis conducted so far depicted general cKSRs in which ≥two kinases phosphorylate the same substrate but not necessarily at the same site. Thus, we went on to extend the analysis to site-specific cKSRs in which the same site is phosphorylated. Also in this case, we observed common convergent motifs in that 1946 (24%) of 7987 Ser/Thr sites or 344 (23%) of 1494 Tyr sites were phosphorylated by ≥two kinases (**Fig. 1D,E**). As for the general cKSRs, a wide range of topologies was observed. We found that 15, 4.7 and 1.7% of substrates are phosphorylated by two, three or four Ser/Thr kinases, and 15, 3.8 and 2.6% of substrates phosphorylated by two, three or four Tyr kinases. Collectively, these results indicate that diverse cKSRs comprise a significant fraction of the human phosphorylation landscape as mapped in the PSP. These results serve as the fundamental dataset that allows delineating key substrates onto

301 which many kinases converge, as well as for a specific site identifying known input kinases
302 (**Supplementary Tables S1-S4**).

303 In an exemplary analysis, we queried the dataset for the presence of reciprocal
304 phosphorylation loops in which the substrate of a kinase is able to phosphorylate that kinase
305 (rendering latter kinase into a cKSR substrate in a reciprocal phosphorylation loop; see
306 **Supplementary Fig. S1** for a schematic of this motif). In the general cKSR dataset, we identified
307 interactions between 33 kinases in 31 unique reciprocal loops (**Supplementary Table S13**). The
308 majority of these interactions (41 of 62) were Ser/Thr phosphorylation events, and included well
309 known feedback loops, such as those upstream the MAPK/ERK pathway and also those in this
310 pathway (e.g., between MEK1 and ERK1). However, the observation that ~half of the identified
311 reciprocal interactions have not been described in the literature previously (**Supplementary**
312 **Table S13**), demonstrates the potential of cKSR data to identify network components with specific
313 topologies for further analysis.

314

315 *Most kinases phosphorylate cKSR substrates*

316 We next investigated how many kinases participate in cKSRs and whether some interaction
317 stoichiometries are more common than others (e.g., are few kinases acting on many substrates,
318 or are many kinases acting on few substrates?). We defined the kinases of interest as those that
319 act on substrates that are phosphorylated by ≥two kinases. We found that this criterion applied to
320 a large fraction of human kinases (87% or 421 of 479 kinases listed in the PSP) (**Fig. 2A-D**). More
321 specifically, of 350 Ser/Thr kinases, 324 or 298 (92 or 85%) were identified to act on general or
322 site-specific cKSR substrates (**Fig. 2A,C**, **Supplementary Tables S5 and S7**). For the 129 Tyr
323 kinases, fractions were somewhat lower but still indicated prominence (61 or 67% were
324 associated with general or site-specific cKSR substrates; **Fig. 2B,D**, **Supplementary Tables S6**
325 **and S8**). We also found that kinase stoichiometries were broadly distributed. Of the identified
326 kinases, most phosphorylated a small number of substrates whilst a small number of kinases
327 acted on many substrates (**Fig. 2A-D**). Collectively, these results indicate that covergent motifs
328 involve a large number of kinases through complex interactions. They allow identifying selected
329 kinases that drive the largest number of phosphorylation events (e.g., the major signaling
330 regulatory Ser/Thr and Tyr kinases ERK2 and SRC; **Supplementary Tables S7 and S8**).

331 We extended this analysis to query if kinases from multiple family subgroups converge on
332 the same substrate or site. Our analysis focused on the major kinase family subgroups AGC,
333 CAMK, CK1, CMGC, RGC, STE, TK, TKL as well as atypical and "other" (Manning *et al.*, 2002).
334 We found that multi-family phosphorylation is common. In the case of general cKSRs, 891 (or
335 70%) of 1268 Ser/Thr substrates, or 27 (or 12%) of 227 Tyr substrates were phosphorylated by
336 kinases of ≥two families (**Supplementary Fig. S2A,B**). In the case of site-specific cKSRs, 791
337 (or 41%) of 1946 Ser/Thr sites ,or 20 (or 5.8%) of 344 Tyr sites were phosphorylated by kinase of
338 ≥two families (**Supplementary Fig. S2C,D**). The lower abundance of Tyr phosphorylation by
339 multiple families needs to be interpreted with caution as it is likely due to the concentration of
340 >90% of Tyr kinases in the TK (tyrosine kinase) group. We further investigated if multiple kinases
341 from the same family subgroup participate in cKSRs. Strikingly, we found that this indeed applies
342 to sizeable fractions of substrates (72.7% for Ser/Thr phosphorylation and 94.7% for Tyr
343 phosphorylation) and sites (77.7% for Ser/Thr phosphorylation and 98% for Tyr phosphorylation)
344 (**Supplementary Figure S3**). These observations motivated the experimental exploration of
345 strategies to dissect the activity of closely related kinases on single substrates (see below).

346 Finally, we also asked if these kinases are co-expressed to relate to biological effects of
347 cKSRs. We analyzed RNA-sequencing data from 1393 human cell lines deposited in the DepMap
348 portal and cancer cell line encyclopedia (Barretina *et al.*, 2012). Similarly to above, we compiled
349 lists of active kinases for either each cKSR substrate or each cKSR phosphorylation site. We then

examined expression levels of these kinases (TPM≥10 in **Fig. 2E**, and also TPM≥5 and 20 in **Supplementary Fig. S4**, all values are given in **Supplementary Tables S9-S12**). As a score for co-expression in each kinase group, we quantified in how many of the 1393 cell lines at least two convergent kinases are expressed (**Fig. 2E, left**). We found that cases of co-expression are generally frequent (**Fig. 2E, right**). On average and for TPM≥10, the identified Ser/Thr kinase groups are co-expressed in >1000 (or >70%) of the analyzed cell lines. Furthermore, only a small number of groups (<4%) were co-expressed more rarely (in <2.5% of cell lines). Similarly, for Tyr kinases, on average the groups were co-expressed in >930 (or >68%) of the analyzed cell lines with <9% of the groups co-expressed more rarely. Albeit co-expression is generally more prominent for Ser/Thr compared to Tyr kinases, these data collectively indicate that not only are large numbers of kinases participants in cKSRs but also that these kinases are in many cases co-expressed. The expression data tabulated in **Supplementary Tables S9-S12** allows identifying kinases and cellular contexts with and without convergence.

Consequences of cKSRs in a prototypical kinase pair

The above analysis points to a significant occurrence of cKSRs. This promoted us to explore the consequences of convergence and to develop a strategy to dissect it for a prototypical kinase pair of the same family with specific inhibitors unavailable. This kinase pair consists of CDK4 and CDK6, two cyclin-dependent kinases that act on the major cell cycle regulator protein RB. We selected the human breast cancer cell line (MCF-7) as the main experimental system as this cell type exhibits high CDK4 levels and low CDK6 levels (TPM_{CDK4}: 170, TPM_{CDK6}: 0.39) (Parry *et al.*, 1999; Yang *et al.*, 2017) and thus offers the possibility to supplement one kinase with the other. Untreated MCF-7 cells exhibit high levels of phosphorylated RB (pRB, Ser780) attributable to CDK4 (**Fig. 3A,B**) (Li et al., 2022; Yang *et al.*, 2017). We tested whether overexpression of CDK6 can elevate pRB levels but observed only a minimal effect (~1.1-fold) in transfected cells. We also examined CDK6 variants harboring two activating mutations, S178P (Bockstaele *et al.*, 2009) or R31C (Hu et al., 2011). The S178P mutant results in the cyclin-independent activation of CDK6 and thus increased cyclin-dependent activity *in vitro* (Bockstaele *et al.*, 2009), whilst the R31C mutation prevents the binding of INK4 protein inhibitors resulting in sustained kinase activity (Hu *et al.*, 2011). Both activating mutations, however, did not result in higher pRB levels compared to WT CDK6 (**Fig. 3A,B**). To test the possibility that D-type cyclins are limiting effects of overexpressed CDK6 (Lin et al., 2001; Parry *et al.*, 1999), we co-transfected Cyclin D3. This D-type cyclin was chosen over D1 and D2 as it is known to promote high levels of kinase activity when in complex specifically with CDK6 (Lin *et al.*, 2001; Parry *et al.*, 1999). Cyclin D3 overexpression resulted in minor increases in pRB levels (~1.2-fold) (**Fig. 3C,D**). The same was observed for CDK6-S178P and -R31C co-transfected with Cyclin D3 (~1.3- and 1.2-fold elevation, resp.) (**Fig. 3C,D**). Collectively, these results indicate that overexpression of CDK6 in cells that exhibit high background activity of the convergent CDK4 does not alter pRB levels.

CDK4/6 inhibition to isolate CDK6 activity

Abemaciclib (LY2835219 [LY]) is an inhibitor of CDK4 and CDK6 with similar half maximal concentrations (IC_{50} 2.0 and 9.9 nM) (Fassl et al., 2022; Gelbert et al., 2014). Previous studies have shown that treatment of MCF-7 cells with LY resulted in the emergence of drug resistance. This resistance was attributed to amplified CDK6 levels resulting in altered cellular inhibitor sensitivity (Cornell et al., 2019; Li *et al.*, 2022; Li et al., 2018; Yang *et al.*, 2017). Based on these observations, we hypothesized that application of LY may reduce background pRB levels in MCF-7 cells and that consequently overexpressed CDK6 may become functionally detectable. We first treated the cells with 0.1 μM LY as this dose was previously shown to be sufficient for inhibition of pRB signals (Yang et al, 2017). In mock-transfected cells this resulted in an almost complete

399 reduction of RB phosphorylation (**Fig. 4A,B**). We next tested cells transfected with Cyclin D3
400 alone, CDK6 alone, CDK6 co-transfected with Cyclin D3, and three CDK6 variants (the loss-of-
401 function variant D163N and above gain of function variants) also co-transfected with Cyclin D3
402 (**Fig. 4A,B**). Strikingly, we found that in the presence of LY overexpression of CDK6 induced pRB
403 levels significantly (~2.5-fold). Furthermore, co-expression of CDK6 with Cyclin D3 resulted in an
404 even greater increase by ~4.1-fold. Similar to our previous experiments, the S178P or R31C
405 variants produced comparable effects to CDK6. The D163N variant as expected showed low pRB
406 levels similar to control cells which demonstrates that effects of ectopic expression of
407 CDK6/Cyclin D3 are kinase-dependent and attributable to active CDK6. Whilst a single dose of
408 LY delivered the desired outcome of isolating CDK6 activity from the CDK4 background, we
409 additionally performed dose response curves (**Fig. 4C,D**). Whilst reduction of pRB levels at
410 increasing concentrations was observed in mock-transfected and Cyclin D3 overexpressing cells,
411 these levels were almost entirely sustained in cells transfected with CDK6/Cyclin D3. A similar
412 selection phenomenon was also observed using Ribociclib ([RI], LEE-011), another CDK4/6
413 inhibitor that is not chemically related to LY (Fassl *et al.*, 2022; Zhang et al., 2014)
414 (**Supplementary Fig. S5**). Overall, these results demonstrate that even in the absence of a
415 specific inhibitor CDK6 activity can be isolated in a convergent motif.

416

417 *In situ assay of CDK6 variants and modulators*

418 We have demonstrated through immunoblotting that CDK6 activity can be quantified in cells using
419 a combination of overexpression and CDK4/6 inhibition. We went on to test if this approach can
420 be applied in a high throughput compatible platform and in the exploration of the function of
421 engineered CDK6 variants. We employed an energy transfer-based assay to detect pRB (Ser780)
422 and total RB levels (**Fig. 5A**). This assay was chosen as it can be used with a greater efficiency
423 than immunoblotting. We first tested the same conditions as above and observed consistent
424 results. CDK6 and activating mutations displayed the greatest fold-increases in pRB levels
425 specifically in the presence of LY (e.g., a >6-fold difference in pRB levels compared to mock
426 inhibitor-treated cells; **Fig. 5A,B**). Also, as observed earlier, CDK6 alone only showed a minor
427 increase and the two activating mutations overall behaved similarly.

428 Given the efficiency of this method, we applied it to study CDK6 function, inhibition and
429 regulation. We first tested whether LY-treated cells overexpressing CDK6/Cyclin D3 can be used
430 to screen for CDK6 inhibitors. Using RI as a test compound, we found that this is indeed the case
431 (**Fig. 5C**). We also examined genetically-engineered versions of CDK6. Fluorescent proteins are
432 commonly fused to enzymes as reporters of cellular levels/location or as functional regulators
433 (Bajar et al., 2016; Rodriguez et al., 2017; Zhou et al., 2017). These modifications can however
434 be associated with a negative impact on protein function (Patel et al., 2019; Snapp, 2009). We
435 introduced sequences encoding the photoactive pdDronpa1 protein (Zhou *et al.*, 2017) at two
436 separate sites of CDK6 to examine if insertion at either site alters activity. pdDronpa1 is a GFP-
437 like protein domain that has been previously used to generate photoswitchable (ps) kinases. Ps-
438 kinases, such as psCDK5, contain pdDronpa1 fused to the N-terminus and inserted in an internal
439 loop (Patel *et al.*, 2019; Zhou *et al.*, 2017). We introduced pdDronpa1 at the N-terminus of CDK6
440 as well as within an internal loop (located between helices α_F and α_G, homologous to insertion in
441 psCDK5 (Zhou *et al.*, 2017), **Supplementary Fig. S6**) as two separate constructs. We found that
442 the N-terminal insertion was well tolerated; however, insertion into the internal loop site completely
443 abolishes activity (**Fig. 5D**). Lastly, we explored the effects of protein modulators of CDK4/6
444 function by co-transfecting the INK4 inhibitor protein p18INK4c (p18). INK4 proteins are known to
445 specifically inhibit and modulate CDK4/6 activity by disrupting the cyclin interaction (Nebenfuehr
446 et al., 2020; Parry *et al.*, 1999). We transfected p18 alone or in combination with CDK6/Cyclin D3
447 or CDK6-R31C/Cyclin D3. The R31C mutant was included as it has previously been shown to
448 reduce binding of INK4 proteins to CDK6 (Hu *et al.*, 2011). Indeed, we found that p18 was able

449 to effectively inhibit CDK6 but unable to inhibit the R31C mutant (**Fig. 5E**). Overall, these findings
450 establish an assay to test genetically modified CDK6 variants and the effect of CDK6 modulators
451 on kinase activity.
452
453
454 **DISCUSSION**

455 The organization of biological systems into networks permits the emergence of complex functions
456 from a finite number of components and interactions. Kinase-substrate interactions have been
457 previously systematically analyzed towards inference of the global network and targeted
458 perturbation of disease-related network elements. The objectives of our study were reductionist
459 as we focused on local motifs and *in situ* assays. Specifically, we addressed three questions
460 through a combination of bioinformatics and experiments: How common are cKSRs in
461 experimentally validated Ser/Thr and Tyr phosphorylation events? What are the most common
462 motif and family subgroup topologies? And, for the prototypical convergent CDK4/6 kinase pair,
463 how can an individual kinase in the motifs be studied experimentally?

464 To answer the first two questions, we systematically mapped human phosphorylation sites
465 from the comprehensive PSP. Information in the experimentally validated PSP reflects on a range
466 of factors that govern specificity in the phosphorylation network, such as evolved substrate
467 recognition capabilities or protein localization in subcellular compartments or on adaptor proteins
468 (Creixell et al., 2018; Ubersax and Ferrell, 2007). We found that a large number of human
469 substrates are phosphorylated by more than one kinase. Furthermore, a majority of human
470 kinases participate in cKSRs, and for both Ser/Thr and Tyr kinases a wide variety of interactions
471 were observed. Finally, in many cases the kinases that act on a common substrate are from the
472 same family subgroup and co-expressed in a large fraction of analyzed cell models. This data
473 collectively points to an abundance of convergent phosphorylation interactions that have the
474 potential to drive multi-site phosphorylation events (associated with amplification, crosstalk and
475 feedback) or redundant phosphorylation events (attributed as a source of diversity and
476 robustness). Our analysis is novel and complementary to kinase-substrate enrichment analysis
477 (Casado et al., 2013), which exploits known KSRs to quantify the strength of these interactions in
478 samples under varying experimental conditions. The objective of our work was to identify the
479 basic properties of cKSRs as a basis for further sequence and coregulation analysis (Creixell *et*
480 *al.*, 2018; Humphrey et al., 2013), or for identification of kinases and substrates involved in
481 relevant network motifs, as demonstrated for fundamental reciprocal phosphorylation events. The
482 observation that related kinases phosphorylate substrates has here motivated the development
483 of the experimental strategy that does not rely on kinase-specific inhibitors.

484 To answer the third question, we studied the convergent CDK4/6 pair under conditions of
485 kinase inhibition. ATP-competitive CDK4/6 inhibitors have led to major improvements in the
486 survival of breast cancer patients. Resistance has emerged in the patient population and, albeit
487 studied intensively, no resistance inducing kinase mutations or substrate protein mutations have
488 been observed. In turn, resistance was attributed to upregulation of CDK6 levels (Cornell *et al.*,
489 2019; Li *et al.*, 2022; Li *et al.*, 2018; Yang *et al.*, 2017). We hypothesized that the interplay of
490 expression level and drug sensitivity can also be explored to design an *in situ* assay for CDK6.
491 We performed these experiments in cells expressing high levels of CDK4 to provide a test bed in
492 which this input entirely masked effects of initial CDK6 overexpression. Ultimately, the generated
493 experimental strategy allowed us to quantify the activity of genetically modified CDK6 kinases,
494 small molecule inhibitors and inhibitory accessory proteins in living cells. The emerging assay
495 complements existing approaches to CDK6 that were in conducted *in vitro* (Bockstaele *et al.*,
496 2009; Li *et al.*, 2022; Soamalala *et al.*, 2020). It also opens the door to more rapid protein
497 engineering approaches that require quantification of cellular CDK6 activity. For instance, we
498 showed that unlike CDK5 (Zhou *et al.*, 2017), CDK6 is not amenable to internal pDronpa1

499 modification. The ability to perform these experiments with inhibitors from different chemical
500 classes (as demonstrated here for LY and RI) allows separating off-target effects (e.g., from
501 inhibition of upstream kinases). Several potential mechanisms for inhibitor resistance in CDK6-
502 amplified cells have been proposed. In the first mechanism, kinases at elevated protein levels are
503 not efficiently inhibited at tuned drug concentrations, and consequently differential signals are
504 recorded between cells with low (e.g., WT cells) or high CDK6 levels (e.g., CDK6 overexpressing
505 cells). In a second mechanism, resistance of CDK6 to inhibitors may be modulated by accessory
506 proteins (Li *et al.*, 2022). Our data suggest that the first mechanism is at play here as we observed
507 a canonical inhibitory function of p18 in the presence of LY leading to reduced pRB levels.

508 Overall, we here analyzed phosphorylation maps using a convergence-centric approach
509 and, in a prototypical experimental system, dissected convergence. Many diverse cKSRs were
510 observed despite the well documented bias of experimental phosphorylation datasets towards
511 well studied kinases (Buljan et al., 2020; Colinge *et al.*, 2014; Invergo and Beltrao, 2018). Our
512 experimental result was achieved even in the absence of kinase-specific inhibitors (e.g., an
513 inhibitor specific for CDK6 over CDK4) or knock-out cell models of the individual converging
514 kinases. Similar limitations may apply to many other scenarios involving convergent kinases. We
515 developed a cellular assay for CDK6 that is desirable as experiments in cells may reflect on a
516 complex natural environment of enzymes and an impact of cellular environment on drug
517 properties. Quite likely redundancy and convergence also exist in other post-translation
518 modification networks, and our work may provide clues as to how to analyze these emerging
519 phenomena.

ACKNOWLEDGEMENTS

We thank Q. Li and S. Chandarlapaty for advice on experimental design, M. Michael and D. Lynn for advice on databases and expression level analysis. This study was supported by grants of the Australian Research Council (FT200100519 and DP200102093, to H.J.), the National Health and Medical Research Council (APP1187638, to H.J.) and a PhD Top-up Scholarship by the Juvenile Diabetes Research Foundation Australia (to C.G.). The Australian Regenerative Medicine Institute is supported by grants from the State Government of Victoria and the Australian Government. The EMBL Australia Partnership Laboratory (EMBL Australia) is supported by the National Collaborative Research Infrastructure Strategy (NCRIS) of the Australian Government. MicroMon of Monash University provided Sanger sequencing services.

AUTHOR CONTRIBUTIONS

Conceptualization, C.G. and H.J.; Formal Analysis, R.S. and H.J.; Funding Acquisition, C.G. and H.J.; Methodology, C.G., R.S. and H.J.; Project Administration, H.J.; Investigation, C.G.; Data curation, C.G., R.S. and H.J.; Supervision, H.J.; Visualization, C.G. and H.J.; Writing - Original Draft, C.G. and H.J.; Writing - Review and Editing, H.J.

DECLARATION OF INTERESTS

The authors declare no competing interests.

541 **Figures**

542

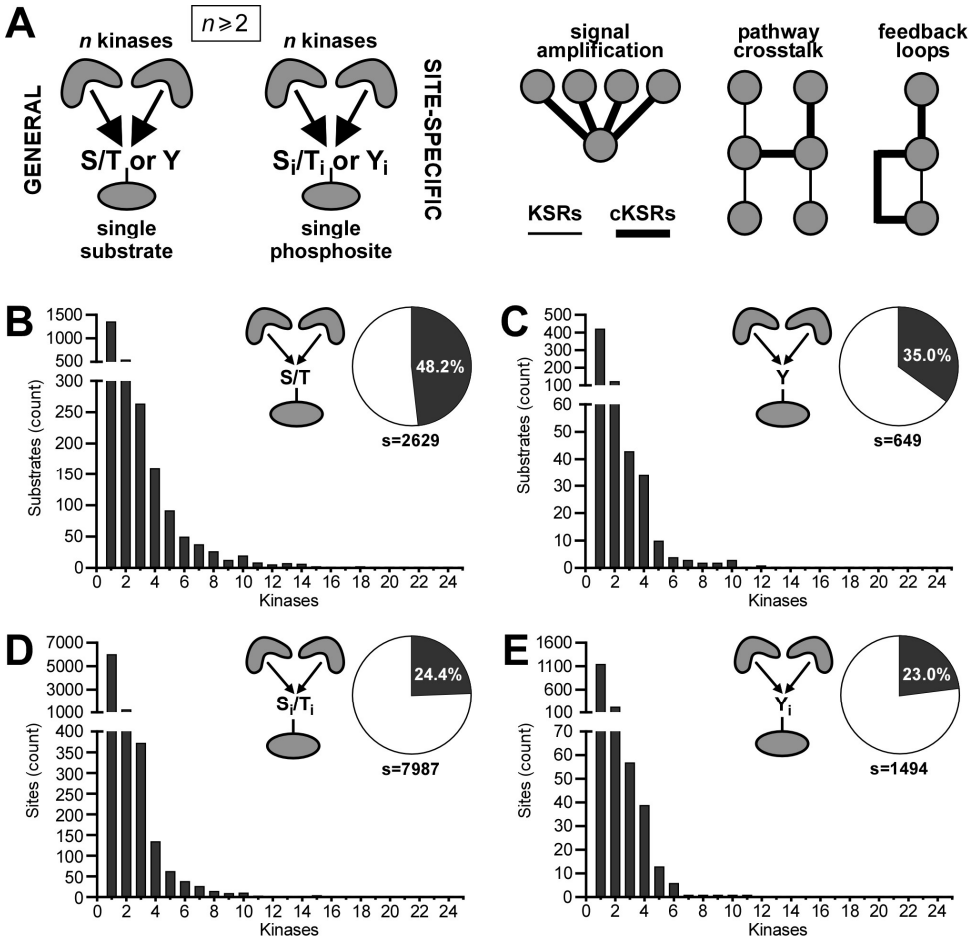

543

544

545 **Figure 1: Substrate-centric analysis of convergent motifs for Ser/Thr and Tyr**
546 **phosphorylation events.** (**A**) cKSRs are defined as kinase-substrate interactions in which ≥two
547 kinase phosphorylate a common substrate (general cKSRs) or a common site on a substrate
548 (site-specific cKSRs). These interactions are involved in, e.g., amplification events, pathway
549 crosstalk and feedback loops. (**B,C**) Distribution histograms of general cKSRs for Ser/Thr
550 phosphorylation (B) and Tyr phosphorylation (C). Bars indicate how many substrates are
551 phosphorylated by the indicated number of kinases. Pie charts indicate the percentage of
552 substrates that are phosphorylated by ≥two kinases and the total number of analyzed substrates
553 (s). (**D,E**) Distribution histograms of site-specific cKSRs for Ser/Thr phosphorylation (D) and Tyr
554 phosphorylation (E). Bars indicate how many sites are phosphorylated by the indicated number
555 of kinases. Pie charts indicated the percentage of sites that are phosphorylated by ≥two kinases
556 and the total number of analyzed sites (s).

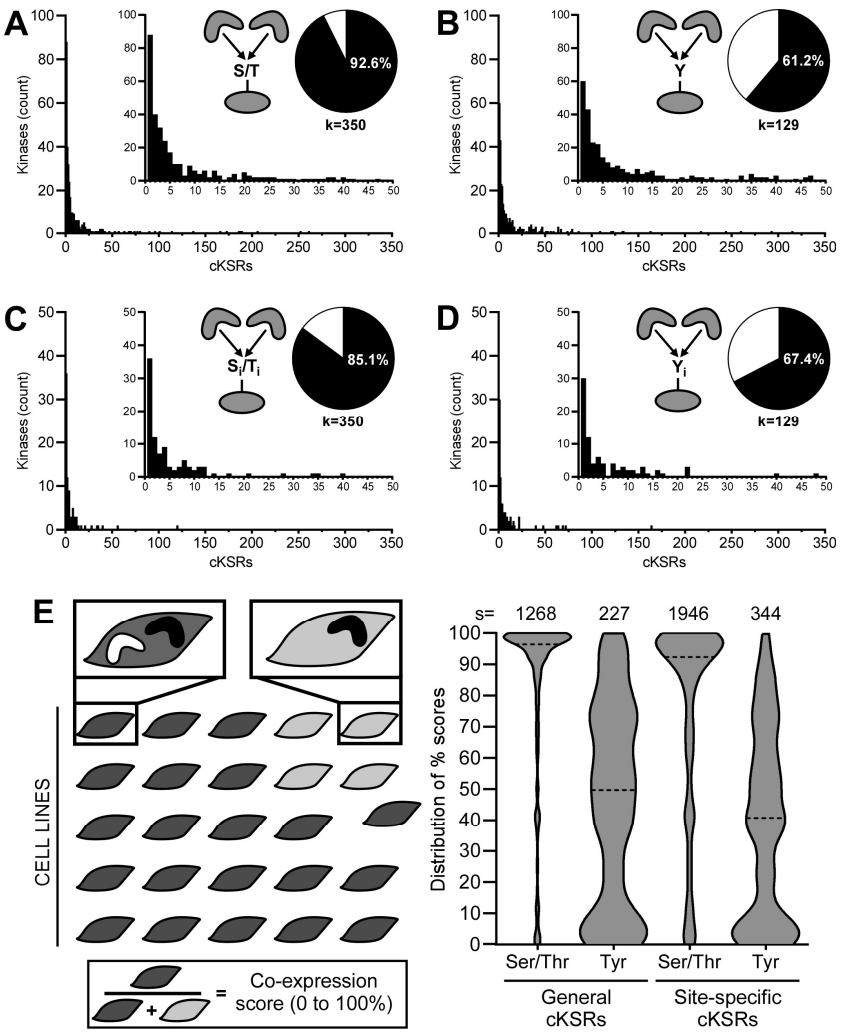

Figure 2: Kinase-centric analysis of convergent motifs for Ser/Thr and Tyr phosphorylation events. (**A,B**) Distribution histograms for Ser/Thr kinases (B) and Tyr kinases (C) in general cKSRs. Bars indicate how many kinases phosphorylate the indicated number of substrates. Pie charts indicate the percentage of kinases that participate in general cKSRs and the total number of kinases (k). (**C,D**) Distribution histograms for Ser/Thr kinases (B) and Tyr kinases (C) in site-specific cKSRs. Bars indicate how many kinases phosphorylate the indicated number of sites. Pie charts indicate the percentage of kinases that participate in site-specific cKSRs and the total number of kinases (k). (**E**) Co-expression analysis of converging kinases in cancer cell lines. For each group of kinases that phosphorylate the same substrate or site, the number of 1393 cancer cell lines that co-express these kinases was counted. From this, a co-expression score was calculated as the ratio of cells with (dark grey) and without (light gray) co-expression. Violin plots summarize the distribution of these scores for the analyzed number of substrates or sites (s) (dashed line: median; TPM threshold: 10).

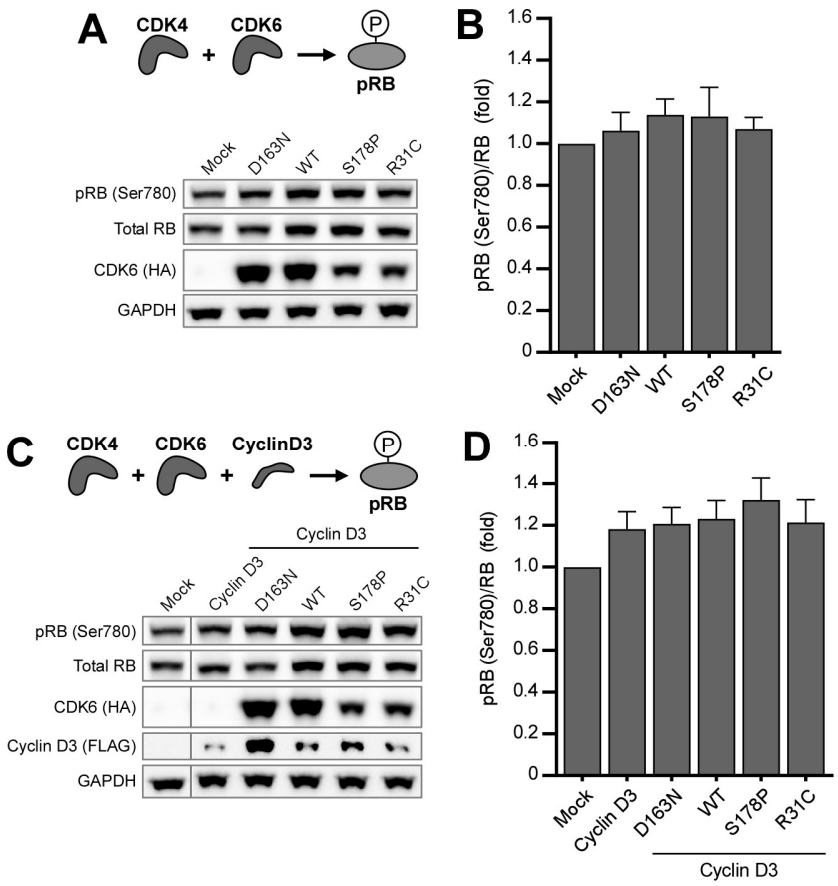

Figure 3: Overexpression of CDK6 and variants does not increase pRB levels. (**A**) Immunoblot analysis of pRB in MCF-7 cells expressing CDK6 and its variants. (**B**) Densitometry analysis of data shown in (A) expressed as a ratio of pRB to total RB. (**C**) Immunoblot analysis of pRB in MCF-7 cells expressing CDK6 and its variants when co-transfected with Cyclin D3. (**D**) Densitometry analysis of data shown (C) expressed as a ratio of pRB to total RB. (A and C) Representative experiments are shown. (B and D) n=3. Data are mean ± SEM.

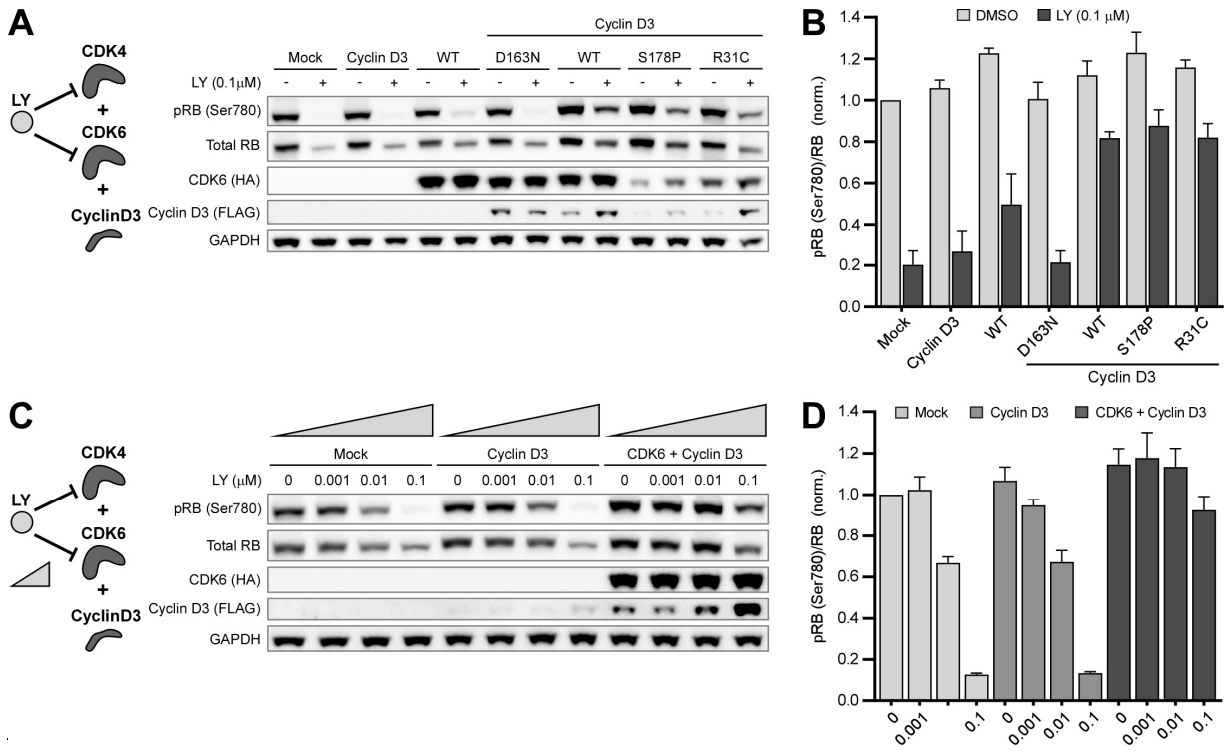

Figure 4: Kinase inhibition with LY reveals CDK6 activity. (**A**) Immunoblot analysis of pRB in MCF-7 cells expressing CDK6 and its variants when co-transfected with Cyclin D3, treated with LY or DMSO. (**B**) Densitometry analysis of data shown in (A) expressed as a ratio of pRB to total RB. (**C**) Immunoblot analysis of pRB in MCF-7 cells expressing CDK6 and Cyclin D3, treated with increasing concentrations of LY. (**D**) Densitometry analysis of data shown in (C) expressed as a ratio of pRB to total RB. (A and C) Representative experiments are shown. (B) n=4 and (C) n=3. Data are mean ± SEM.

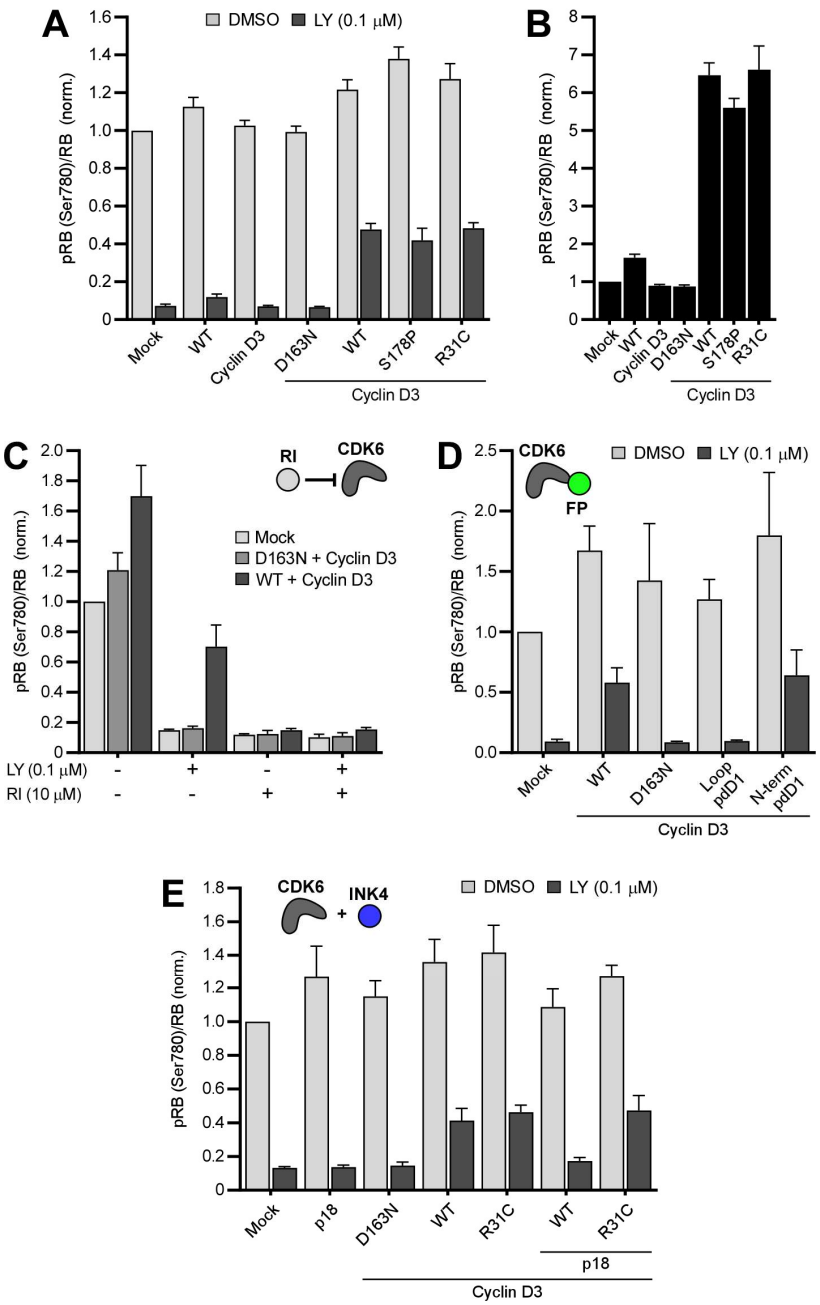

Figure 5: Energy transfer-based assay of CDK6 variants, inhibitors and modulators. (**A**) Ratios of pRB to total RB for MCF-7 cells expressing CDK6 and its variants co-transfected with Cyclin D3. (**B**) LY-treated conditions from (A) normalized to mock LY-treated control. (**C**) Ratios for cells expressing constructs and treated with different combinations of LY and RI. (**D**) Ratios for cells expressing CDK6 containing pdDronpa1 insertions within an internal loop (loop pdD1) or at the N-terminus (N-term pdD1). (**E**) Ratios for cells expressing $p18^{INK4c}$ (p18) in combination with CDK6 or R31C variant and Cyclin D3. (A-E) n=3. Data are mean ± SEM.

598 **Supplementary Information**

599

600 **Supplementary Tables S1 to S12:** Please see separate Supplementary Data (Excel format).

601 **Supplementary Table S13: Reciprocal phosphorylation loops.** Loops of the topology shown
602 in Supplementary Fig. S1 were identified in the cKSR data and literature searched for prior
603 mention (see Methods for details).
604

Kinase A	Kinase B	Reaction A to B	Reaction B to A	Prior mention
Abl	MST1	Tyr	Ser/Thr	N
Akt1	CDK2	Ser/Thr	Ser/Thr	N
Akt1	CK2A1	Ser/Thr	Ser/Thr	N
Akt1	GSK3A	Ser/Thr	Ser/Thr	N
Akt1	mTOR	Ser/Thr	Ser/Thr	Y
Akt1	PIKFYE	Ser/Thr	Ser/Thr	N
Arg	PDGFRB	Tyr	Tyr	N
ASK1	PDK1	Ser/Thr	Ser/Thr	Y
Btk	ITK	Tyr	Tyr	Y
Btk	TEC	Tyr	Tyr	Y
CDK1	CDK7	Ser/Thr	Ser/Thr	N
CDK1	Chk1	Ser/Thr	Ser/Thr	Y
CDK1	CK2A1	Ser/Thr	Ser/Thr	N
CDK1	Wee1	Ser/Thr	Tyr	Y
CDK2	CDK7	Ser/Thr	Ser/Thr and Tyr	Y
Chk2	TTK	Ser/Thr	Ser/Thr	N
CK2A1	ERK2	Ser/Thr	Ser/Thr	N
EGFR	ERK1	Ser/Thr and Tyr	Ser/Thr	Y
EGFR	ERK2	Ser/Thr and Tyr	Ser/Thr	Y
ERK1	Lck	Ser/Thr	Tyr	Y
ERK1	MEK1	Ser/Thr	Ser/Thr and Tyr	Y
ERK2	MEK1	Ser/Thr	Ser/Thr and Tyr	Y
FAK	Ret	Tyr	Tyr	Y
GSK3B	Src	Ser/Thr and Tyr	Tyr	N
ITK	TEC	Tyr	Tyr	Y
MEK1	RAF1	Ser/Thr	Ser/Thr	Y
mTOR	p70S6K	Ser/Thr	Ser/Thr	Y
PKCD	Src	Ser/Thr	Tyr	Y

605

Supplementary Table S14: Protein sequences of WT CDK6 and engineered CDK6 variants.
Color code: Start codon. HA tag. WT human CDK6. Linkers. pdDronpa1.

CDK6	MYPYDVPDYAEKDGLCRADQQYECVAEIGEGAYGKVFKARDLKNGGRFVALKRVRVQTGEEGMPLSTIREVAV LRHLETFEHPNVVRLFDVCTVSRTDRETKLTLVFEHVDQDLTTYLDKVPEPGVPTETIKDMMFQLLRGLDFLH SHRVVHRDLKPQNILVTSSGQIKLADFGLARIYSFQMALTSVVVTLWYRAPEVLLQSSYATPVDLWSVGCIFA EMFRRKPLFRGSSDVDQLGKILDVIGLPGEEDWPRDVALPRQAFHSKSAQPIEKFVTDIDELGKDLLLKCLTF NPAKRISAYSALSHPYFQDLERCKENLDSHLPPSQNTSELNTA
pdDronpa1-CDK6 (N-term pdD1)	MYPYDVPDYASVIKPDMKIKLRMEGAVNGHPFAIEGVGLGKPFEGKQSIDLKVKEGGPLPFAYDILTTAFCYG NRVFAKYPENIVDYFKQSFPEGYSWERSMNYEDGGICNATNDITLDGDCYIYEIRFRGTNFPANGPVMQKRTV KWEPSTENLYVRDGVLKGDVVMALSLEGGGHYRCDFKTTYKAKKVVQLPDYHFVDHHIEIKSHDKDYSNVNLH EHAEAHSELPRQAKGLKGSGEKDGLCRADQQYECVAEIGEGAYGKVFKARDLKNGGRFVALKRVRVQTGEEGM PLSTIREVAVLRHLETFEHPNVVRLFDVCTVSRTDRETKLTLVFEHVDQDLTTYLDKVPEPGVPTETIKDMMF QLLRGLDFLHSHRVVHRDLKPQNILVTSSGQIKLADFGLARIYSFQMALTSVVVTLWYRAPEVLLQSSYATPV DLWSVGCIFAEMFRRKPLFRGSSDVDQLGKILDVIGLPGEEDWPRDVALPRQAFHSKSAQPIEKFVTDIDELG KDLLLKCLTFNPAKRISAYSALSHPYFQDLERCKENLDSHLPPSQNTSELNTA
CDK6-internal-pdDronpa1 (loop pdD1)	MYPYDVPDYAEKDGLCRADQQYECVAEIGEGAYGKVFKARDLKNGGRFVALKRVRVQTGEEGMPLSTIREVAV LRHLETFEHPNVVRLFDVCTVSRTDRETKLTLVFEHVDQDLTTYLDKVPEPGVPTETIKDMMFQLLRGLDFLH SHRVVHRDLKPQNILVTSSGQIKLADFGLARIYSFQMALTSVVVTLWYRAPEVLLQSSYATPVDLWSVGCIFA EMFRRKPLFRGTGGSVIKPDMKIKLRMEGAVNGHPFAIEGVGLGKPFEGKQSIDLKVKEGGPLPFAYDILTTA FCYGNRVFAKYPENIVDYFKQSFPEGYSWERSMNYEDGGICNATNDITLDGDCYIYEIRFRGTNFPANGPVMQ KRTVKWEPSTENLYVRDGVLKGDVVMALSLEGGGHYRCDFKTTYKAKKVVQLPDYHFVDHHIEIKSHDKDYSN VNLHEHAEAHSELPRQAKRTSSDVDQLGKILDVIGLPGEEDWPRDVALPRQAFHSKSAQPIEKFVTDIDELGK DLLLKCLTFNPAKRISAYSALSHPYFQDLERCKENLDSHLPPSQNTSELNTA

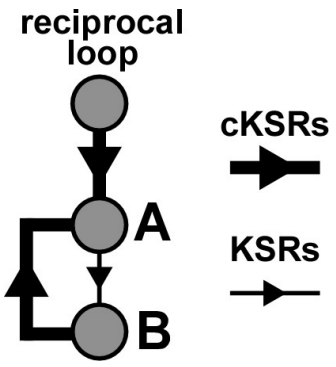

Supplementary Figure S1: Topology of reciprocal phosphorylation loops. The general cKSR dataset was analyzed to identify all kinases A that receive two inputs and whose substrates B are phosphorylating these kinases reciprocally. The identified kinase pairs are listed in Supplementary Table S13.

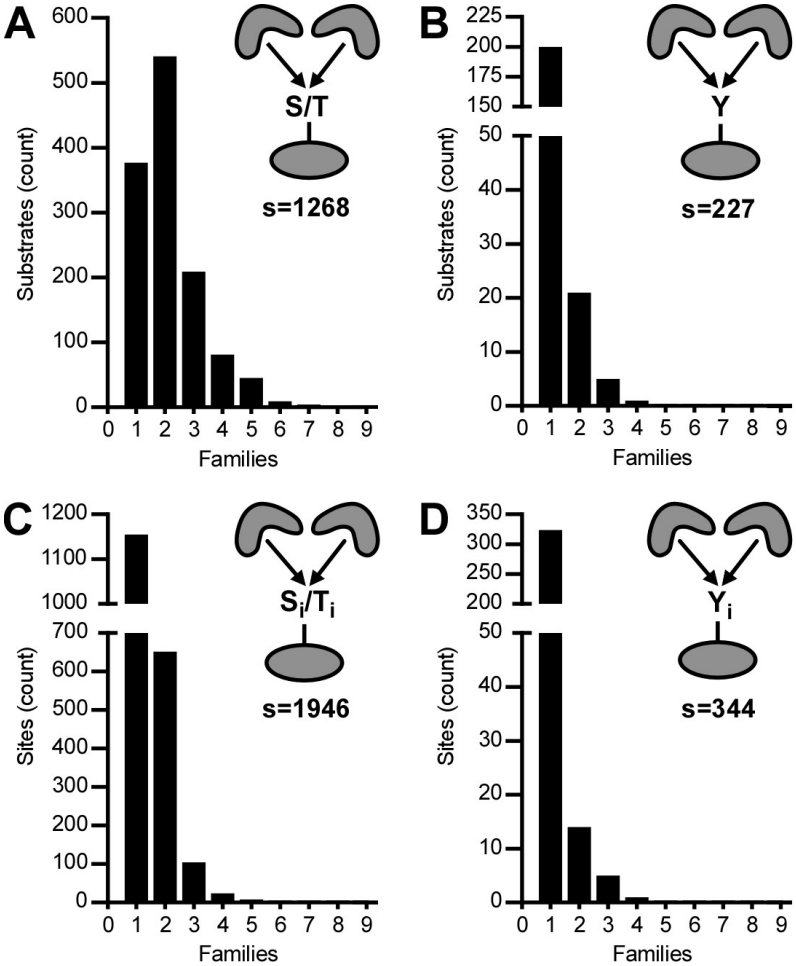

616

617

618 **Supplementary Figure S2: Distribution histograms of kinase families participating in**
619 **convergent Ser/Thr phosphorylation (A, C) and Tyr phosphorylation (B, D).** Bars indicate
620 the number of substrates (A, B) or sites (C, D) that are phosphorylated by members of
621 theindicated number of kinase families. s: Analyzed number of substrates or sites.

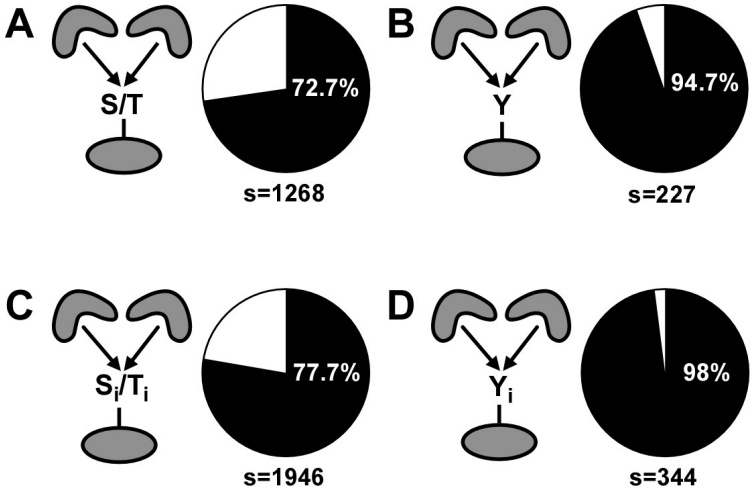

Supplementary Figure S3: Occurrence of phosphorylation events that include ≥two kinases from the same family subgroup. Pie charts indicating the percentage of substrates that are phosphorylated by ≥two kinases from at least one family subgroup, for general and site-specific Ser/Thr phosphorylation (A, C) and general and site-specific Tyr phosphorylation (B,D). s: Analyzed number of substrates or sites.

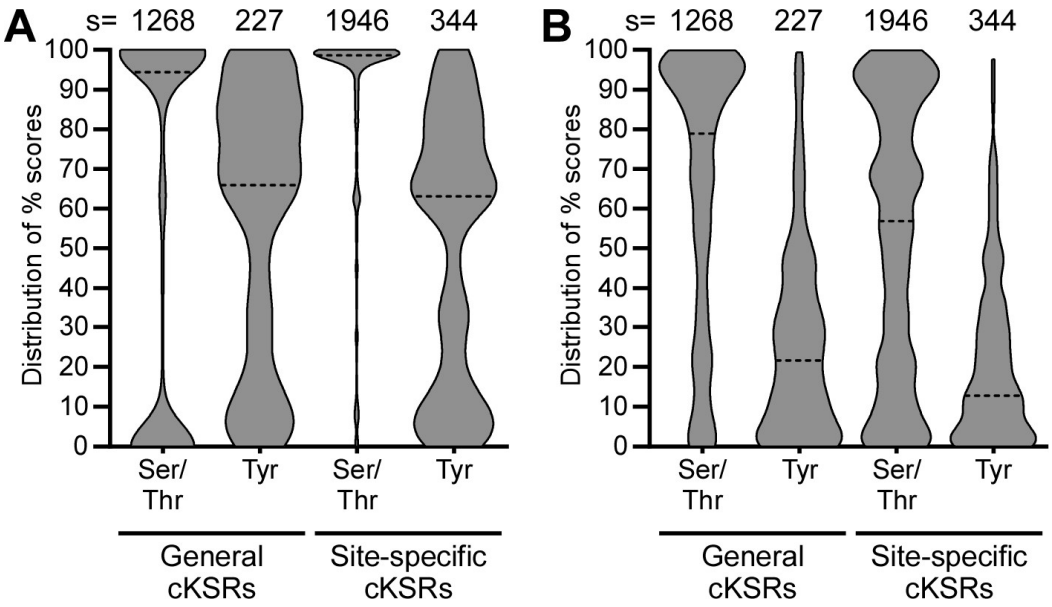

Supplementary Figure S4: Co-expression analysis at different TPM thresholds. (**A**) TPM threshold of 5. (**B**) TPM threshold of 20. Co-expression scores and median (dashed line) are defined as in Fig. 2. s: Analyzed number of substrates or sites.

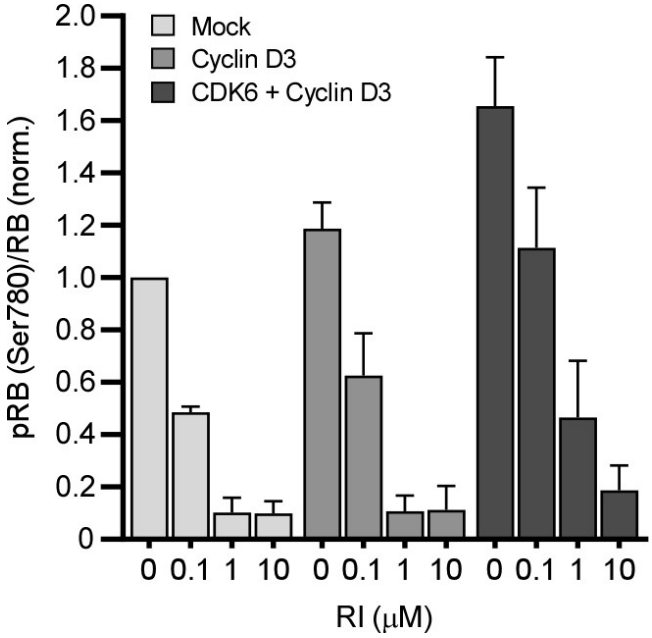

634

635

636 **Supplementary Figure S5: Kinase inhibition with RI reveals CDK6 activity.** Energy transfer-
637 based assay to detect ratios of pRB to total RB for MCF-7 cells expressing CDK6 and Cyclin D3
638 treated with increasing concentrations of RI. n=3. Data are mean ± SEM.

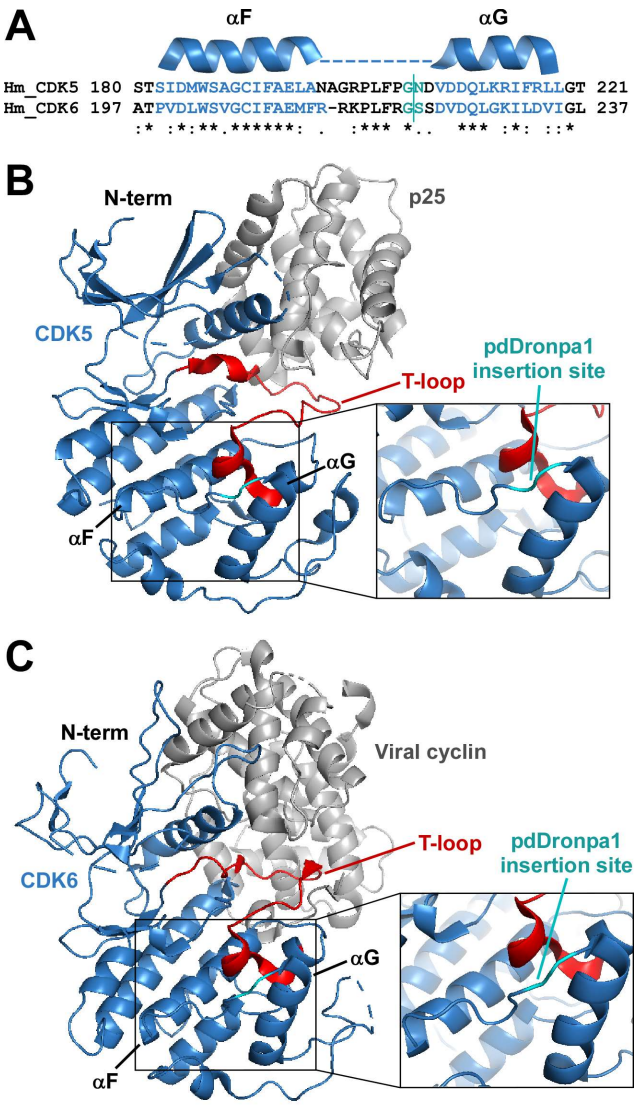

Supplementary Figure S6: Analogous insertion sites of pDronpa1 in CDK5 and CDK6. (**A**) Protein sequence alignment of human CDK5 and CDK6. pdDronpa1 internal loop insertion site highlighted in cyan (for CDK5, the insertion is equivalent to that of psCDK5 (Zhou *et al.*, 2017)). (**B** and **C**) CDK5-p25 and CDK6-viral cyclin complex structures with the insertion sites highlighted (PDB-IDs: 1H4L for CDK5 and 1JOW for CDK6).

646 **References**

647 Aebersold, R., and Mann, M. (2016). Mass-spectrometric exploration of proteome structure and
648 function. Nature *537*, 347-355.

649 Alganem, K., Hamoud, A.R., Creeden, J.F., Henkel, N.D., Imami, A.S., Joyce, A.W., Ryan,
650 V.W., Rethman, J.B., Shukla, R., O'Donovan, S.M., et al. (2022). The active kinome: The
651 modern view of how active protein kinase networks fit in biological research. Curr Opin
652 Pharmacol *62*, 117-129.

653 Anders, L., Ke, N., Hydbring, P., Choi, Y.J., Widlund, H.R., Chick, J.M., Zhai, H., Vidal, M., Gygi,
654 S.P., and Braun, P. (2011). A systematic screen for CDK4/6 substrates links FOXM1
655 phosphorylation to senescence suppression in cancer cells. Cancer Cell *20*, 620-634.

656 Bajar, B.T., Lam, A.J., Badiee, R.K., Oh, Y.-H., Chu, J., Zhou, X.X., Kim, N., Kim, B.B., Chung,
657 M., and Yablonovitch, A.L. (2016). Fluorescent indicators for simultaneous reporting of all four
658 cell cycle phases. Nat Methods *13*, 993-996.

659 Barretina, J., Caponigro, G., Stransky, N., Venkatesan, K., Margolin, A.A., Kim, S., Wilson, C.J.,
660 Lehár, J., Kryukov, G.V., and Sonkin, D. (2012). The cancer cell line encyclopedia enables
661 predictive modelling of anticancer drug sensitivity. Nature *483*, 603-607.

662 Blain, S. (2008). Switching cyclin D-Cdk4 kinase activity on and off. Cell Cycle *7*, 892-898.

663 Bockstaele, L., Bisteau, X., Paternot, S., and Roger, P.P. (2009). Differential regulation of
664 cyclin-dependent kinase 4 (CDK4) and CDK6, evidence that CDK4 might not be activated by
665 CDK7, and design of a CDK6 activating mutation. Mol Cell Biol *29*, 4188-4200.

666 Bockstaele, L., Kooken, H., Libert, F., Paternot, S., Dumont, J.E., De Launoit, Y., Roger, P.P.,
667 and Coulonval, K. (2006). Regulated activating Thr172 phosphorylation of cyclin-dependent
668 kinase 4 (CDK4): its relationship with cyclins and CDK “inhibitors”. Mol Cell Biol *26*, 5070-5085.

669 Budde, A., Schneiderhan-Marra, N., Petersen, G., and Brüne, B. (2005). Retinoblastoma
670 susceptibility gene product pRB activates hypoxia-inducible factor-1 (HIF-1). Oncogene *24*,
671 1802-1808.

672 Buljan, M., Ciuffa, R., van Drogen, A., Vichalkovski, A., Mehnert, M., Rosenberger, G., Lee, S.,
673 Varjosalo, M., Pernas, L.E., Spegg, V., et al. (2020). Kinase Interaction Network Expands
674 Functional and Disease Roles of Human Kinases. Mol Cell *79*, 504-520 e509.

675 Casado, P., Rodriguez-Prados, J.C., Cosulich, S.C., Guichard, S., Vanhaesebroeck, B., Joel,
676 S., and Cutillas, P.R. (2013). Kinase-substrate enrichment analysis provides insights into the
677 heterogeneity of signaling pathway activation in leukemia cells. Sci Signal *6*, rs6.

678 Chen, P.L., Riley, D.J., Chen-Kiang, S., and Lee, W.H. (1996a). Retinoblastoma protein directly
679 interacts with and activates the transcription factor NF-IL6. Proc Natl Acad Sci U S A *93*, 465-
680 469.

681 Chen, P.L., Riley, D.J., Chen, Y., and Lee, W.H. (1996b). Retinoblastoma protein positively
682 regulates terminal adipocyte differentiation through direct interaction with C/EBPs. Genes Dev
683 *10*, 2794-2804.

684 Chen, Y.A., and Eschrich, S.A. (2014). Computational methods and opportunities for
685 phosphorylation network medicine. Transl Cancer Res *3*, 266-278.

686 Cheng, M., Olivier, P., Diehl, J.A., Fero, M., Roussel, M.F., Roberts, J.M., and Sherr, C.J.
687 (1999). The p21(Cip1) and p27(Kip1) CDK 'inhibitors' are essential activators of cyclin D-
688 dependent kinases in murine fibroblasts. EMBO J *18*, 1571-1583.

689 Colinge, J., César-Razquin, A., Huber, K., Breitwieser, F.P., Májek, P., and Superti-Furga, G.
690 (2014). Building and exploring an integrated human kinase network: global organization and
691 medical entry points. J Proteomics *107*, 113-127.

692 Cornell, L., Wander, S.A., Visal, T., Wagle, N., and Shapiro, G.I. (2019). MicroRNA-mediated
693 suppression of the TGF-β pathway confers transmissible and reversible CDK4/6 inhibitor
694 resistance. Cell Rep *26*, 2667-2680.e2667.

695 Creixell, P., Pandey, J.P., Palmeri, A., Bhattacharyya, M., Creixell, M., Ranganathan, R.,
696 Pincus, D., and Yaffe, M.B. (2018). Hierarchical organization endows the kinase domain with
697 regulatory plasticity. Cell Syst *7*, 371-383 e374.

698 Dall'Acqua, A., Sonego, M., Pellizzari, I., Pellarin, I., Canzonieri, V., D'Andrea, S., Benevol, S.,
699 Sorio, R., Giorda, G., Califano, D., et al. (2017). CDK6 protects epithelial ovarian cancer from
700 platinum-induced death via FOXO3 regulation. EMBO Mol Med *9*, 1415-1433.

701 Fassl, A., Geng, Y., and Sicinski, P. (2022). CDK4 and CDK6 kinases: From basic science to
702 cancer therapy. Science *375*, eabc1495.

703 Fisher, R.P. (2005). Secrets of a double agent: CDK7 in cell-cycle control and transcription. J
704 Cell Sci *118*, 5171-5180.

705 Gelbert, L.M., Cai, S., Lin, X., Sanchez-Martinez, C., Del Prado, M., Lallena, M.J., Torres, R.,
706 Ajamie, R.T., Wishart, G.N., and Flack, R.S. (2014). Preclinical characterization of the CDK4/6
707 inhibitor LY2835219: in-vivo cell cycle-dependent/independent anti-tumor activities alone/in
708 combination with gemcitabine. Invest New Drugs *32*, 825-837.

709 Hirai, H., Roussel, M.F., Kato, J.Y., Ashmun, R.A., and Sherr, C.J. (1995). Novel INK4 proteins,
710 p19 and p18, are specific inhibitors of the cyclin D-dependent kinases CDK4 and CDK6. Mol
711 Cell Biol *15*, 2672-2681.

712 Hornbeck, P.V., Zhang, B., Murray, B., Kornhauser, J.M., Latham, V., and Skrzypek, E. (2015).
713 PhosphoSitePlus, 2014: mutations, PTMs and recalibrations. Nucleic Acids Res *43*, D512-
714 D520.

715 Hu, M.G., Deshpande, A., Schlichting, N., Hinds, E.A., Mao, C., Dose, M., Hu, G.-f., Van Etten,
716 R.A., Gounari, F., and Hinds, P.W. (2011). CDK6 kinase activity is required for thymocyte
717 development. Blood *117*, 6120-6131.

718 Humphrey, S.J., Yang, G., Yang, P., Fazakerley, D.J., Stockli, J., Yang, J.Y., and James, D.E.
719 (2013). Dynamic adipocyte phosphoproteome reveals that Akt directly regulates mTORC2. Cell
720 Met *17*, 1009-1020.

721 Hydbring, P., Malumbres, M., and Sicinski, P. (2016). Non-canonical functions of cell cycle
722 cyclins and cyclin-dependent kinases. Nat Rev Mol Cell Biol *17*, 280-292.

723 Invergo, B.M., and Beltrao, P. (2018). Reconstructing phosphorylation signalling networks from
724 quantitative phosphoproteomic data. Essays Biochem *62*, 525-534.

725 Jinno, S., Hung, S.C., and Okayama, H. (1999). Cell cycle start from quiescence controlled by
726 tyrosine phosphorylation of Cdk4. Oncogene *18*, 565-571.

727 Kaelin, W.G., Jr. (1999). Functions of the retinoblastoma protein. Bioessays *21*, 950-958.

728 Kitagawa, M., Higashi, H., Jung, H.-K., Suzuki Takahashi, I., Ikeda, M., Tamai, K., Kato, J.-Y.,
729 Segawa, K., Yoshida, E., and Nishimura, S. (1996). The consensus motif for phosphorylation by
730 cyclin D1-Cdk4 is different from that for phosphorylation by cyclin A/E-Cdk2. EMBO J *15*, 7060-
731 7069.

732 Lemeer, S., and Heck, A.J. (2009). The phosphoproteomics data explosion. Curr Opin Chem
733 Biol *13*, 414-420.

734 Li, Q., Jiang, B., Guo, J., Shao, H., Del Priore, I.S., Chang, Q., Kudo, R., Li, Z., Razavi, P., and
735 Liu, B. (2022). INK4 tumor suppressor proteins mediate resistance to CDK4/6 kinase inhibitors.
736 Cancer Discov *12*, 356-371.

737 Li, Z., Razavi, P., Li, Q., Toy, W., Liu, B., Ping, C., Hsieh, W., Sanchez-Vega, F., Brown, D.N.,
738 and Paula, A.F.D.C. (2018). Loss of the FAT1 tumor suppressor promotes resistance to CDK4/6
739 inhibitors via the hippo pathway. Cancer Cell *34*, 893-905. e898.

740 Lin, J., Jinno, S., and Okayama, H. (2001). Cdk6-cyclin D3 complex evades inhibition by
741 inhibitor proteins and uniquely controls cell's proliferation competence. Oncogene *20*, 2000-
742 2009.

743 Malumbres, M. (2014). Cyclin-dependent kinases. Genome Biol *15*, 1-10.

744 Malumbres, M., and Barbacid, M. (2001). To cycle or not to cycle: a critical decision in cancer.
745 Nat Rev Cancer *1*, 222-231.

746 Malumbres, M., Sotillo, R.o., Santamaría, D., Galán, J., Cerezo, A., Ortega, S., Dubus, P., and
747 Barbacid, M. (2004). Mammalian cells cycle without the D-type cyclin-dependent kinases Cdk4
748 and Cdk6. Cell *118*, 493-504.

749 Manning, G., Whyte, D.B., Martinez, R., Hunter, T., and Sudarsanam, S. (2002). The protein
750 kinase complement of the human genome. Science *298*, 1912-1934.

751 Nebenfuehr, S., Kollmann, K., and Sexl, V. (2020). The role of CDK6 in cancer. Int J Cancer
752 *147*, 2988-2995.

753 Parry, D., Mahony, D., Wills, K., and Lees, E. (1999). Cyclin D-CDK subunit arrangement is
754 dependent on the availability of competing INK4 and p21 class inhibitors. Mol Cell Biol *19*, 1775-
755 1783.

756 Patel, A.L., Yeung, E., McGuire, S.E., Wu, A.Y., Toettcher, J.E., Burdine, R.D., and
757 Shvartsman, S.Y. (2019). Optimizing photoswitchable MEK. Proc Natl Acad Sci U S A *116*,
758 25756-25763.

759 Paternot, S., Coulonval, K., Dumont, J.E., and Roger, P.P. (2003). Cyclic AMP-dependent
760 phosphorylation of cyclin D3-bound CDK4 determines the passage through the cell cycle
761 restriction point in thyroid epithelial cells. J Biol Chem *278*, 26533-26540.

762 Pellerano, M., and Morris, M.C. (2021). Fluorescent peptide biosensors for probing CDK kinase
763 activity in cell extracts. Methods Mol Biol *2329*, 39-50.

764 Riley, N.M., and Coon, J.J. (2016). Phosphoproteomics in the Age of Rapid and Deep Proteome
765 Profiling. Anal Chem *88*, 74-94.

766 Rodriguez, E.A., Campbell, R.E., Lin, J.Y., Lin, M.Z., Miyawaki, A., Palmer, A.E., Shu, X.,
767 Zhang, J., and Tsien, R.Y. (2017). The growing and glowing toolbox of fluorescent and
768 photoactive proteins. Trends Biochem Sci *42*, 111-129.

769 Rubin, S.M. (2013). Deciphering the retinoblastoma protein phosphorylation code. Trends
770 Biochem Sci *38*, 12-19.

771 Schachter, M.M., Merrick, K.A., Larochelle, S., Hirschi, A., Zhang, C., Shokat, K.M., Rubin,
772 S.M., and Fisher, R.P. (2013). A Cdk7-Cdk4 T-loop phosphorylation cascade promotes G1
773 progression. Mol Cell *50*, 250-260.

774 Sherr, C.J., Beach, D., and Shapiro, G.I. (2016). Targeting CDK4 and CDK6: From discovery to
775 therapy. Cancer Discov *6*, 353-367.

776 Sherr, C.J., and Roberts, J.M. (1999). CDK inhibitors: positive and negative regulators of G1-
777 phase progression. Genes Dev *13*, 1501-1512.

778 Snapp, E.L. (2009). Fluorescent proteins: a cell biologist's user guide. Trends Cell Biol *19*, 649-
779 655.

780 Soamalala, J., Diot, S., Pellerano, M., Blanquart, C., Galibert, M., Jullian, M., Puget, K., and
781 Morris, M.C. (2020). Fluorescent peptide biosensor for probing CDK6 activity in lung cancer cell
782 extracts. ChemBioChem.

783 Tigan, A., Bellutti, F., Kollmann, K., Tebb, G., and Sexl, V. (2016). CDK6—a review of the past
784 and a glimpse into the future: from cell-cycle control to transcriptional regulation. Oncogene *35*,
785 3083-3091.

786 Ubersax, J.A., and Ferrell, J.E., Jr. (2007). Mechanisms of specificity in protein phosphorylation.
787 Nat Rev Mol Cell Biol *8*, 530-541.

788 Van, T.N.N., Pellerano, M., Lykaso, S., and Morris, M.C. (2014). Fluorescent protein biosensor
789 for probing CDK/cyclin activity in vitro and in living cells. ChemBioChem *15*, 2298-2305.

790 Wang, H., Nicolay, B.N., Chick, J.M., Gao, X., Geng, Y., Ren, H., Gao, H., Yang, G., Williams,
791 J.A., and Suski, J.M. (2017). The metabolic function of cyclin D3–CDK6 kinase in cancer cell
792 survival. Nature *546*, 426-430.

793 Yang, C., Li, Z., Bhatt, T., Dickler, M., Giri, D., Scaltriti, M., Baselga, J., Rosen, N., and
794 Chandarlapaty, S. (2017). Acquired CDK6 amplification promotes breast cancer resistance to
795 CDK4/6 inhibitors and loss of ER signaling and dependence. Oncogene *36*, 2255-2264.

796 Zhang, Y.-X., Sicinska, E., Czaplinski, J.T., Remillard, S.P., Moss, S., Wang, Y., Brain, C., Loo,
797 A., Snyder, E.L., and Demetri, G.D. (2014). Antiproliferative effects of CDK4/6 inhibition in
798 CDK4-amplified human liposarcoma in vitro and in vivo. Mol Cancer Ther *13*, 2184-2193.

799 Zhou, X.X., Fan, L.Z., Li, P., Shen, K., and Lin, M.Z. (2017). Optical control of cell signaling by
800 single-chain photoswitchable kinases. Science *355*, 836-842.